sustainability

MDPI

Article

Soil Arsenic Toxicity Impact on the Growth and C-Assimilation of *Eucalyptus nitens*

José C. Ramalho [1,2,*], João Pelica [3], Fernando C. Lidon [2], Maria M. A. Silva [2], Maria M. Simões [2], Mauro Guerra [4] and Fernando H. Reboredo [2,*]

[1] PlantStress & Biodiversity Lab, Centro de Estudos Florestais (CEF), Instituto Superior Agronomia (ISA), Universidade de Lisboa (ULisboa), Quinta do Marquês, Av. República, 2784-505 Oeiras e Tapada da Ajuda, 1349-017 Lisboa, Portugal
[2] GeoBioTec, Departamento de Ciências da Terra, Faculdade de Ciências e Tecnologia, Universidade NOVA de Lisboa, Campus da Caparica, 2829-516 Caparica, Portugal
[3] Departamento Ciências da Terra, Faculdade de Ciências e Tecnologia, Universidade Nova de Lisboa, Campus da Caparica, 2829-516 Caparica, Portugal
[4] LIBPHYS, Departamento de Física, Faculdade de Ciências e Tecnologia, Universidade NOVA de Lisboa, Campus da Caparica, 2829-516 Caparica, Portugal
* Correspondence: cochichor@mail.telepac.pt (J.C.R.); fhr@fct.unl.pt (F.H.R.)

Abstract: The selection of adequate plants that can cope with species that can live in contaminated/degraded and abandoned mining areas is of utmost importance, especially for environmental management and policymakers. In this framework, the use of a fast-growing forestry species, such as *Eucalyptus nitens*, in the recovery of arsenic (As) from artificially contaminated soils during a long-term experiment was studied. Roots can accumulate to levels ranging between 69.8 and 133 μg g^{-1} for plants treated with 100 and 200 μg As mL^{-1}, respectively, while leaves between 9.48 μg g^{-1} (200 As) and 15.9 μg g^{-1} (100 As) without apparent morphological damage and toxicity symptoms. The C-assimilation machinery performance revealed a gradual impact, as evaluated through some gas exchange parameters such as the net photosynthetic rate (P_n), stomatal conductance to H_2O (g_s), and transpiration rate (E), usually with the greater impacts at the highest As concentration (200 As), although without significantly impacting the PSII performance. The As effects on the uptake and translocation of Ca, Fe, K, and Zn revealed two contrasting interferences. The first one was associated with Zn, where a moderate antagonism was detected, whereas the second one was related to Fe, where a particular enrichment in leaves was noted under both As treatments. Thus, it seems to exist a synergistic action with an impact on the levels of the photosynthetic pigments in As-treated plant leaves, compared with control plants. *E. nitens* must be considered as an alternative when phytoremediation processes are put into practice in our country, particularly in areas with cool climatic conditions.

Keywords: arsenic toxicity; *Eucalyptus nitens*; nutrient uptake; photosynthesis tolerance; photosynthetic pigments; phytoremediation

Citation: Ramalho, J.C.; Pelica, J.; Lidon, F.C.; Silva, M.M.A.; Simões, M.M.; Guerra, M.; Reboredo, F.H. Soil Arsenic Toxicity Impact on the Growth and C-Assimilation of *Eucalyptus nitens*. *Sustainability* **2023**, *15*, 6665. https://doi.org/10.3390/su15086665

Academic Editors: Shahabaldin Rezania, Ewa Wojciechowska and Nicole Nawrot

Received: 22 February 2023
Revised: 11 March 2023
Accepted: 27 March 2023
Published: 14 April 2023

1. Introduction

The heavy metal and metalloid contamination of both agricultural and natural ecosystems by anthropogenic activities is a major concern due to the effects on both human life and biodiversity. Therefore, the control and reduction of emissions is the focus of international and European Union action [1].

The evaluation of the contamination degree of heavy metals in different compartments, such as agricultural soils [2], water basin sediments [3–5], or atmosphere [6], has been the target of different researchers, mainly due to anthropogenic activities in both developed and developing countries. Within industrial activities, mining is one that greatly contributes with large inputs of heavy metals to the aquifers and soils. In fact, the presence of huge mine

tailings enriched with heavy metals and metalloids might contribute to soil and aquifer contamination through rainwater percolation [7], plus aerial dispersion to surrounding areas, leading to a possible transfer to the food chain.

The disposal of huge quantities of extractive waste in Europe is a major concern since ca. 900,000 tons of extractive waste are generated annually, being stored in tailing facilities or ponds, corresponding to 26% of the EU's current waste output [8]. The very high contamination of soils situated around mine dump areas was evaluated regarding the mobilization of different heavy metals to green beans, courgettes, oranges, and figs [2]. The authors concluded that the regular intake of these edible plants might pose a great risk to human health due to the high Cu levels detected, beyond the adverse effects on cell plant physiology, mainly on crop germination, growth, photosynthesis, and antioxidant activity [9–11].

Human exposure from contaminated soils around gold mine tailings dumps, and consequent metal and metalloid exposure, clearly indicates a greater health risk (including cancer) to children than to adults [12]. Similarly, tailings resulting from non-ferrous mining areas are a major concern related to heavy metal contamination of farmland soils in China, where children are the most vulnerable group to non-carcinogenic risk compared to adults, especially when dealing with As [13].

The Directive 2006/21/EC3 on the management of waste from the extractive industries provides guidance on actions to prevent or reduce (as far as possible) the adverse effects on the environment and the resulting risks to human health [14]. In order to mitigate the effects, several approaches can be taken, such as Remediation, which is focused on the removal of pollutants from a closed mining site in order to clean up the contaminated land to safe levels, and Rehabilitation with the aim of returning the land to some degree of its former state [15].

In that sense, the use of phytoremediation, as a low-cost process, can be implemented in order to alleviate contaminant dispersion through an efficient root system uptake, as observed in abandoned mining sites [16,17], although the success of this process depends of the selected plant species and soil characteristics. For example, when testing the phytoextraction capabilities of six different tree species cultivated on mining sludge, it was observed that *Acer platanoides* L. was the best choice to carry out effective phytoextraction [18] whereas *Acer pseudoplatanus* L., *Betula pendula* Roth, *Quercus robur* L., *Tilia cordata* Miller, *Ulmus laevis* Pall. were able to survive, accumulating As, Cd, Cu, Pb, and Tl mainly in the roots, and Zn was mainly in the shoots.

In Portugal, the evaluation of phytoremediation capabilities relies mostly on natural wild species, which can accumulate contaminants in variable concentrations [19,20]; most of them are herbaceous or shrubs, which are not as efficient as we expect. In that sense, some studies have been performed in order to identify fast-growing ligneous species (trees) with greater suitability for phytoremediation than herbaceous species, namely based on their longevity, greater biomass accumulation, and extensive rooting traits [21]. The genus *Eucalyptus* sp. has been successfully used worldwide in both in vivo [22,23] and in vitro assays [24,25] in soils contaminated with heavy metals. Eucalyptus plantations, especially *E. globulus* are extensively spread in Portugal, for pulp production, mainly in 10–12 years rotations and currently occupying 812,000 ha in the mainland [26]. Despite *E. globulus* being the main species used in afforestation, *Eucalyptus nitens* is under evaluation due to its high tolerance to frost [27], which is a strong handicap to the former species. In this context, it can be used as an alternative in some regions of Portugal where winter temperatures are too low.

In natural conditions, plants can be exposed to multiple abiotic stresses. The plant vigor status and global functioning are frequently assessed through the performance of the C-assimilation machinery [28–30] to detect interferences leading to growth decline and yield reduction. Thus, this type of approach can also be used in vitro conditions. In this framework and taking into account the prevalent levels of As in agricultural soils surrounding the Neves-Corvo mining area [2], an experiment with *Eucalyptus nitens* growing in soil

artificially contaminated with As for six months was implemented. This assay aimed to verify the *E. nitens* plant's capability to uptake and translocate As to the different organs, the As impact on C-assimilation performance (evaluated through leaf gas exchanges and chlorophyll a fluorescence parameters), and the As interference on the uptake and balance of other important nutrients.

2. Materials and Methods

2.1. Plant Material and Experimental Conditions

Eucalyptus nitens Deane and Maiden plants, ca. 11 months of age, were taken from the nursery Altri Florestal S.A. and placed in 5 L pots, using 3 L of SIRO Universal substrate (pH: 5.5–6.5; humidity: 50–60%, electrical conductivity: 0.6–1.2 (mS m^{-1}), N: 80–150 mg L^{-1}; P_2O_5: 80–150 mg L^{-1}; K_2O: 300–500 mg L^{-1}; organic matter > 70%). Potted plants were then transferred for acclimation to natural conditions in Campus da Caparica, Portugal (Gps—38° 39′ 41, 5″ N, 9° 12′ 24, 0″ W) during four months (from September to December). The maximum and minimum mean air temperatures during that period were 21.9 °C and 10.1 °C, respectively [31], whereas the mean values of total annual rainfall reached 600 mm.

Three distinct groups of 24 plants, i.e., a control group and two As treatments, were formed. Arsenic was added to the soil in January as $NaAsO_2$, soluble in 100 ml bi-distilled water in two distinct concentrations, 100 (100 As) or 200 (200 As) µg As mL^{-1}, while control plants received the same volume of bi-distilled water only. After soil contamination at the end of January 2015 (T0 moment), plant and soil analyses were carried out every two months, i.e., by the end of March (T1), May (T2), and July 2015 (T3), ca. 2, 4, and 6 months after soil contamination. The bioaccumulation factor (BAF) indicates the capability of a plant to uptake a metal, in this case As, from soil and was calculated with the following equations: $BAF = C_{leaf}/C_{soil}$ and $BAF = C_{root}/C_{soil}$, where C represents the metal concentrations in leaves, roots, and soil.

2.2. Growth Parameters and Photosynthetic Pigment Evaluation

Some growth parameters, such as the specific leaf area ratio (SLA), the leaf weight ratio (LWR), and the leaf area ratio (LAR), were evaluated [32] were evaluated along the experimental period. The photosynthetic pigments (total chlorophyll and total carotenoids) were extracted from leaf discs (1.5 cm^2) in 80% acetone, determined spectrophotometrically, and calculated according to the formulae of Lichtenthaler [33]. In each case, four replicates were used for the determination of the above-mentioned parameters.

2.3. Leaf Gas Exchange Monitoring

Net photosynthetic rates (P_n), stomatal conductance to H_2O vapor (g_s), and transpiration rate (Tr) were evaluated and obtained with a portable open-system infrared gas analyzer (CIRAS 3, PP Systems, USA) on 1st April, 2nd June, and 30th July. Measurements were performed under photosynthetic steady-state after at least 2 h of illumination under local environmental conditions, except for the CO_2 that was provided internally by the device (ca. 390–400 µL L^{-1} and irradiance), and irradiance that was controlled to reach ca. 1500 µmol Q m^{-2} s^{-1}, of natural solar irradiance along the entire experiment.

2.4. Chlorophyll a Fluorescence Analysis

The assessment of chlorophyll (Chl.) fluorescence parameters were performed on the same dates and conditions mentioned for leaf gas exchange in plant leaves, using a PAM-2000 system (H. Walz, Effeltrich, Germany) [34,35] and the formulae discussed elsewhere [36–38].

Briefly, minimum fluorescence (F_0) and maximal PSII photochemical efficiency (F_v/F_m) were obtained at predawn under dark-adapted conditions. Additionally, several other parameters were obtained under steady-state photosynthetic conditions (ca. 1500 µmol Q m^{-2} s^{-1} of solar irradiance): the photosystem II (PSII) photochemical efficiency under light (F_v'/F_m'), the photochemical quenching based on the concept of interconnected PSII

antennae (q_L) [36,38], the predictor of the rate constant of PSII inactivation (F_s/F_m') [39], the estimates of the photosynthetic quantum yields of (A) non-cyclic electron transfer ($Y_{(II)}$), (B) photoprotective regulated energy dissipation of PSII ($Y_{(NPQ)}$), and (C) non-regulated energy dissipation of PSII as heat/fluorescence ($Y_{(NO)}$) [36,40]. Finally, it was calculated the PSII photoinhibition indexes [41,42] included chronic photoinhibition (PI_{Chr}) and total photoinhibition ($PI_{Total} = PI_{Chr} + PI_{Dyn}$).

2.5. Elemental Quantification in Soil and Plant Organs

For determination of As, Ca, Fe, K, and Zn, the plants were withdrawn from the pots, washed carefully with tap and deionized water to remove soil and dust particles, and afterward splinted into roots, stems, and leaves, which were dried at 60 °C for 72 h until constant weight. Thereafter, plant samples were powdered and stored. Soil drying followed a process similar to that of plant material before analysis.

The elemental determination in soil, roots, stems, and leaves were performed in triplicate for each treatment, in a total of 36 samples per collection date, through an X-ray Analyser (Thermo Scientific, Niton model XL3t 950 He GOLDD+, USA) following the Environmental Protection Agency (EPA) method 6200 [43]. Detection limits using the optimum "mining" mode for a period of 120s under high purity helium (He) were: As = 5 μg g^{-1}; Ca = 350 μg g^{-1}; Fe = 25 μg g^{-1}; K = 500 μg g^{-1}; Zn = 6 μg g^{-1}; K = 500 μg g^{-1}. Soil reference materials—NRCan Till-1 [44] and plant reference materials (Orchard Leaves—SRM 1571) were used at the beginning of the analytical process and after every five samples. The recovery values ranged between 91% and 96%.

2.6. Micro-Energy Dispersive X-ray Fluorescence (μ-EDXRF)

Given the high limits of detection of portable devices for some elements in light matrices, all the stems and leaves were also analyzed using a benchtop micro X-Ray Fluorescence spectrometer (μ-EDXRF). The spectrometer used in this work was the Bruker M4 Tornado^{TM} system that features an air-cooled X-ray tube with an Rh anode and a silicon drift detector, XFlash^{TM}, with a 30 mm^2 sensitive area and an energy resolution of 142 eV@5.9 keV. The system also features pollycapillary X-ray optics that focuses the beam onto a 22 μm spot in diameter for the Rh Kα line energy. All measures were performed at 50 kV and 600 μA with a detector dead time of around 1%.

All samples were dehydrated and reduced to powder form in a mortar and pressed under two tons in a hydraulic press to form a cylindrical pellet, 20 ± 1 mm in diameter. This pellet was then glued onto a myllar sheet and placed directly under the X-ray beam for analysis. Each sample was fabricated in triplicate for statistical purposes. Quantification of the obtained spectra was performed with the in-built ESPRIT software, and the method reliability was checked against a set of standard reference materials, namely Orchard Leaves (NBS 1571) and Sea Lettuce (BCR-279). The recovery values for As were 115% for NBS 1571 and 99% for BCR-279, which puts the certified value within the measured average ± standard deviation concentration interval. The detection limit of this spectrometer for As in these matrices is around 3 μg/g [45,46].

2.7. Statistical Analysis

Data were statistically analyzed with a comparison of means with two-way ANOVA, considering differences over time or between As treatments. This was followed by Tukey's HSD test for mean comparisons using the SPSS statistical package (Version 14.0). A 95% confidence level was adopted for all tests.

3. Results

3.1. Arsenic Accumulation

Among plant organs, roots showed the greatest As accumulation during the experiment, although the pattern of accumulation was similar in both plants treated with 100 and 200 μg As mL^{-1}. From March till May, the levels in the roots increase (Table 1), decreasing

to approximately 70 μg g^{-1} and 106 μg g^{-1} in July for plants treated with 100 As and 200 As, respectively.

Table 1. Changes in As content in different organs of *E. nitens* plants submitted to 100 or 200 μg As mL^{-1} and in the substrata, expressed as μg g^{-1}. Bioaccumulation Factor (BAF) was also determined.

		100 As	200 As	100 As-BAF	200 As-BAF
March-T1	Leaf	*BDL*	14.0 ± 0.6 a	———	Leaf/soil = 0.54
	Stem	*BDL*	*BDL*		
	Root	72.8 ± 14.5 a,s	118 ± 32.0 a,r	Root/soil = 4.11	Root/soil = 4.56
	Soil	17.7 ± 6.49 br	25.9 ± 4.55 ar		
May-T2	Leaf	10.0 ± 0.5 br	13.3 ± 0.4 ar	Leaf/soil = 0.29	Leaf/soil = 0.32
	Stem	3.24 ± 0.25 *	4.30 ± 0.22 *		
	Root	90.1 ± 26.7 a,s	133 ± 18.4 a,r	Root/soil = 2.64	Root/soil = 3.18
	Soil	34.1 ± 6.37 ar	41.8 ± 17.3 ar		
July-T3	Leaf	15.9 ± 1.6 ar	9.48 ± 2.22 as	Leaf/soil = 0.80	Leaf/soil = 0.30
	Stem	5.04 ± 0.17 *	7.25 ± 0.36 a		
	Root	69.8 ± 14.1 a,s	106 ± 5.0 a,r	Root/soil = 3.52	Root/soil = 3.38
	Soil	19.8 ± 6.08 br	31.4 ± 6.06 ar		

For each case, different letters after the mean values ±standard deviation (n = 3) express significant differences over time (a, b) or between As treatments in each date (r, s); (*) Concentrations determined by μ-EDXRF; *BDL* = Below the Detection Limit; BAF = Bioaccumulation Factor; Arsenic was never found in control plants.

The accumulation of As in the leaves of plants treated with 200 As slightly decreased from March till May (14 μg g^{-1} vs. 13 μg g^{-1}, respectively), decreasing to 9.5 by the end of July. Conversely, plants treated with 100 As do not exhibit detectable As levels in March but gradually raised until 16 μg g^{-1} in July (Table 1).

The accumulation of As in the stems was only detected in May in both treatments with levels < 5.0 μg g^{-1} As, slightly increasing till July, reaching 5.04 μg g^{-1} in plants treated with 100 As, and 7.2 μg g^{-1} in plants treated with 200 As. Regarding the substrata, As reaches a maximum of 41.8 μg g^{-1} in May, with the 200 As treatment declining in July to 31.4 μg g^{-1}. Soils contaminated with 100 As also exhibited the highest levels in May (34.1 μg g^{-1}) declining to 19.8 μg g^{-1} in July. The bioaccumulation factors or BAF revealed values < 1 in the case of As accumulation in the leaves versus uptake from substrata, while the equivalent values for roots range between 2.64 and 4.56, indicating that below-ground organs had a high capability of extract As from the artificially contaminated soil (Table 1).

3.2. Plant Growth and Foliar Traits

All studied leaf traits (Figure 1), which included specific leaf area (SLA), leaf weight ratio (LWR), and leaf area ratio (LAR), showed a declining pattern throughout the experiment. That was significant in SLA for control plants only by July, for control and 200 As plants in LWR in May and July, and for all plants for LAR also in the latest two evaluation dates. However, there were no significant differences between As and control plants on all evaluation dates, thus denoting an absence of As impact. Regarding photosynthetic pigments, both chlorophyll and carotenoid concentrations appear to be stimulated by the levels of As used since 100 and 200 As treatments always had higher levels than control ones (Figure 2).

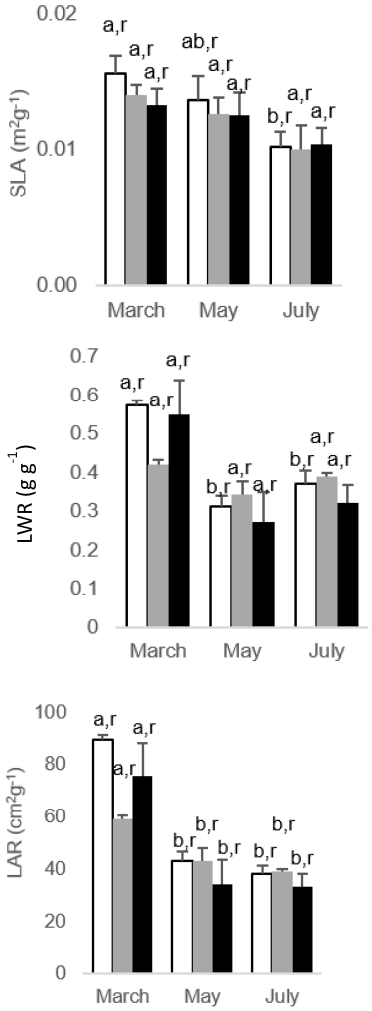

Figure 1. Alterations regarding the leaf traits, specific leaf area (SLA), leaf weight ratio (LWR), and leaf area ratio (LAR), in *Eucalyptus nitens*, along the experimental For each parameter, different letters after the mean values ± standard error (n = 4) express significant differences over time (a, b) or between As treatments within each date (r), considering the control (white), 100 As (grey), and 200 As (black) treatments, and the data points T1(March), T2 (May), and T3 (July).

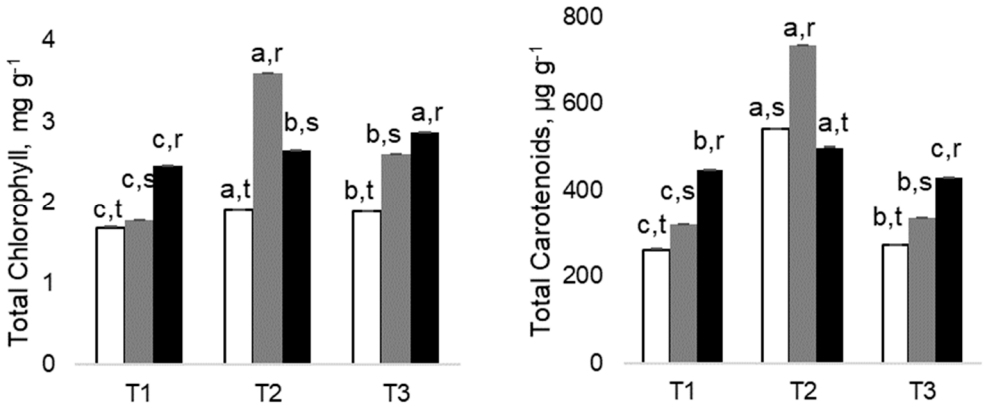

Figure 2. Changes in Total Chlorophyll and Total Carotenoids in *Eucalyptus nitens*, along the experimental. Different letters after the mean values ± standard error (n = 4) express significant differences over time (a, b, c) or between As treatments within each date (r, s, t), considering the control (white), 100 As (grey), and 200 As (black) treatments, and the data points T1(March), T2 (May) and T3 (July).

3.3. As Impact in Leaf Gas Exchanges

The As impact was mostly absent by the first date of evaluation in P_n, g_s, and E (Figure 3). However, with the persistence of As submission in time, significant impacts were observed in May and July for the three parameters, as compared with their respective controls. The impacts were also dose-related, with the greatest reductions observed with un the 200 As plants and with 100 As counterparts showing an intermediate decline. Therefore, maximal differences to the control values were observed in the latest evaluation date (July) when 200 As showed declines of 60%, 72%, and 67% for P_n, g_s, and E, respectively.

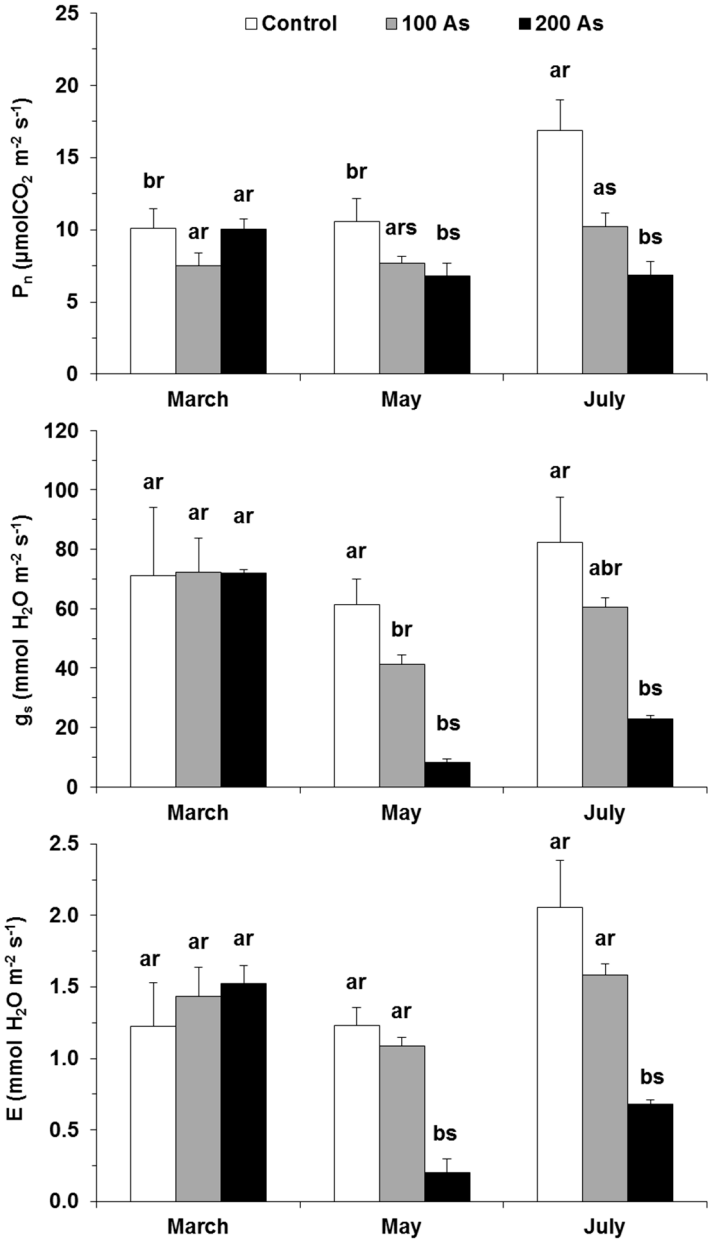

Figure 3. Changes in the leaf gas exchange parameters—net photosynthetic rate (P_n), stomatal conductance to H_2O vapor (g_s), and the transpiration rate (E) in *E. nitens* plants along the experiment. For each parameter, different letters after the mean values ± standard error (n = 4–6) express significant differences over time (a, b) or between As treatments within each date (r, s), considering the Control (white), 100 As (grey), and 200 As (black) treatments, and the data points of March (T1), May (T2), and July (T3).

3.4. As Impact in Chlorophyll a Fluorescence

Although some impact tendencies were already observed in May (T2), significant As impacts were mostly observed in the plants submitted to the high dose treatment (200 As) and in the last date for the PSII functioning/dissipation processes as compared with the control. More in detail, F_0 was not modified by As treatments within each date, but the 200 As plants showed an increased value by the last evaluation time in comparison with the first one, similar to the impact on the maximal photochemical efficiency of PSII (F_v/F_m)—Table 2.

Table 2. Variation of leaf chlorophyll a fluorescence data along the experiment with *E. nitens* plants submitted to 0 (Control), 100 (100 As), or 200 (200 As) μg As mL^{-1} treatment. The parameters included the minimal fluorescence, F_o, maximal photochemical efficiency of PSII, F_v/F_m, the estimate of the quantum yield of non-cyclic electron transport, $Y_{(II)}$, the quantum yield of regulated energy dissipation of PSII, $Y_{(NPQ)}$, the quantum yield of non-regulated energy (heat and fluorescence) dissipation of PSII, $Y_{(NO)}$, the photoprotective sustained thermal dissipation, q_N, photochemical quenching based on the concept of interconnected PSII antennae, q_L, the actual PSII photochemical efficiency of energy conversion (F_v'/F_m'), the predictor of the rate constant of PSII inactivation (F_s/F_m'), as well as the dynamic photoinhibition (PI_{Dyn}), chronic photoinhibition (PI_{Chr}), and total photoinhibition (PI_{Total}).

Treatment	March (T1)		May (T2)		July (T3)	
			F_0			
Control	0.18 ±	0.00 a,r	0.18 ±	0.01 a,r	0.22 ±	0.01 a,r
100 As	0.18 ±	0.00 a,r	0.18 ±	0.00 a,r	0.22 ±	0.02 a,r
200 As	0.20 ±	0.01 b,r	0.20 ±	0.01 b,s	0.28 ±	0.02 a,r
			F_v/F_m			
Control	0.80 ±	0.02 a,r	0.82 ±	0.01 a,r	0.77 ±	0.01 a,r
100 As	0.77 ±	0.02 a,r	0.81 ±	0.00 a,r	0.77 ±	0.02 a,r
200 As	0.80 ±	0.00 a,r	0.80 ±	0.01 a,r	0.70 ±	0.02 a,s
			$Y_{(II)}$			
Control	0.26 ±	0.05 a,r	0.28 ±	0.03 a,r	0.27 ±	0.05 a,r
100 As	0.23 ±	0.05 b,r	0.8 ±	0.03 a,s	0.16 ±	0.02 ab,s
200 As	0.21 ±	0.01 a,r	0.19 ±	0.05 a,rs	0.14 ±	0.00 a,s
			$Y_{(NPQ)}$			
Control	0.32 ±	0.06 a,rs	0.54 ±	0.03 a,r	0.41 ±	0.08 a,s
100 As	0.24 ±	0.06 a,s	0.55 ±	0.06 a,r	0.54 ±	0.03 a,rs
200 As	0.37 ±	0.03 b,r	0.56 ±	0.05 b,r	0.59 ±	0.04 a,r
			$Y_{(NO)}$			
Control	0.42 ±	0.07 a,r	0.17 ±	0.01 b,r	0.32 ±	0.04 a,r
100 As	0.50 ±	0.04 a,r	0.27 ±	0.04 b,r	0.30 ±	0.02 b,r
200 As	0.42 ±	0.04 a,r	0.25 ±	0.09 b,r	0.27 ±	0.03 b,r
			q_N			
Control	0.64 ±	0.07 b,r	0.84 ±	0.01 a,r	0.71 ±	0.11 ab,r
100 As	0.53 ±	0.10 b,r	0.75 ±	0.06 ab,r	0.81 ±	0.04 a,r
200 As	0.71 ±	0.03 a,r	0.76 ±	0.12 a,r	0.84 ±	0.03 a,r
			q_L			
Control	0.36 ±	0.06 a,r	0.34 ±	0.02 a,r	0.45 ±	0.10 a,r
100 As	0.31 ±	0.05 a,r	0.14 ±	0.06 a,s	0.29 ±	0.02 a,s
200 As	0.35 ±	0.04 a,r	0.22 ±	0.08 a,rs	0.29 ±	0.03 a,s

Table 2. *Cont.*

Treatment	March (T1)		May (T2)		July (T3)	
			F_v'/F_m'			
Control	0.49 ±	0.04 a,r	0.54 ±	0.03 a,r	0.47 ±	0.10 a,r
100 As	0.47 ±	0.06 ab,r	0.61 ±	0.03 a,r	0.41 ±	0.03 b,r
200 As	0.43 ±	0.02 ab,r	0.57 ±	0.08 a,r	0.37 ±	0.03 b,r
			F_s/F_m'			
Control	0.75 ±	0.06 a,r	0.72 ±	0.03 a,r	0.73 ±	0.05 a,s
100 As	0.77 ±	0.05 a,r	0.82 ±	0.02 a,r	0.84 ±	0.01 a,rs
200 As	0.80 ±	0.01 a,r	0.81 ±	0.03 a,r	0.86 ±	0.00 a,r
			PI_{Chr}			
Control	7.12 ±	1.57 a,r	5.54 ±	1.80 a,r	7.28 ±	0.66 a,r
100 As	5.16 ±	1.76 a,r	6.69 ±	2.47 a,r	7.33 ±	1.79 a,r
200 As	6.30 ±	1.23 a,r	7.18 ±	2.30 a,r	7.62 ±	2.31 a,r
			PI_{Dyn}			
Control	39.4 ±	12.1 a,r	35.3 ±	3.7 a,r	37.9 ±	12.4 a,r
100 As	35.8 ±	6.8 ab,r	24.5 ±	9.3 b,r	45.3 ±	5.9 a,r
200 As	45.5 ±	2.3 a,r	28.9 ±	11.2 a,r	41.3 ±	3.3 a,r
			PI_{Total}			
Control	40.5 ±	5.4 a,r	35.3 ±	3.7 a,r	42.6 ±	12.7 a,r
100 As	41.6 ±	7.0 ab,r	24.5 ±	4.7 b,r	49.6 ±	4.1 a,r
200 As	46.9 ±	2.1 ab,r	30.4 ±	9.3 b,r	54.4 ±	3.1 a,r

For each parameter, different letters after the mean values ± standard error (n = 8) express significant differences over time (a, b) or between As treatments within each date (r, s).

The energy flow through photochemistry can be assessed by the estimate of the quantum yield of non-cyclic electron transport ($Y_{(II)}$) and the photochemical quenching (q_L). Both parameters were moderately impacted by both As doses in May but showed significant negative impacts in 100 and 200 As plants in July, without differences between As doses. These impacts were not accompanied by significant declines in the actual PSII photochemical efficiency of energy conversion (F_v'/F_m'), regardless of As dose. Still, a tendency to a lower value in the 200 As plants were observed by the last evaluation date, in accordance with a significant increase in the PSII inactivation (F_s/F_m') and a consistent rise (non-significantly) of the chronic photoinhibition (PI_{Chr}), and total photoinhibition (PI_{Total}) indexes in these same plants.

Nevertheless, the absence of greater impacts in the PSII functioning in 200 As plants on the same date (July) was likely associated with the increase of photoprotective processes, as reflected in the rises of the estimate of regulated energy dissipation of PSII ($Y_{(NPQ)}$), and the non-photochemical quenching (q_N) (significantly only for the first), whereas non-regulated energy dissipation processes ($Y_{(NO)}$) did not show any increase, thus denoting that deleterious photo inhibitory impacts were not present (as compared with the control plants).

For most of the above-studied parameters, the 100 As usually displayed an intermediate value between control and 200 As plants in the last evaluation date (either closer to control or to the 200 As treatment values), thus somewhat revealing a relationship between the applied As doses and the impacts in the performance of the photosynthetic apparatus. Finally, the dynamic photoinhibition (PI_{Dyn}) index showed only minor fluctuations, both during the experiment and between treatments.

3.5. Elemental Accumulation

3.5.1. Calcium

At the moment of T1 (March), the uptake of Ca by the roots was reduced in the presence of As-control plants contained 3.89%, while both As-treated plants had 2.89% (Figure 4). A similar pattern was also noted for the stems, but not in leaves where the concentrations of Ca were not significantly different. By the end of the experiment, control plants exhibited the highest Ca concentration in all the organs, although the differences

in the mean values had not been significantly different. However, it must be emphasized that the highest As treatment (200 As) corresponds to the lowest Ca concentrations in the roots and stems while maintaining a similar Ca level in the leaves compared with plants treated with half of the As concentration (Figure 4). The highest concentrations were generally observed in the roots regardless of the treatments, with levels in general above 3.5%, but only in leaves; it was observed an increase in Ca content from March to July, irrespective of treatments.

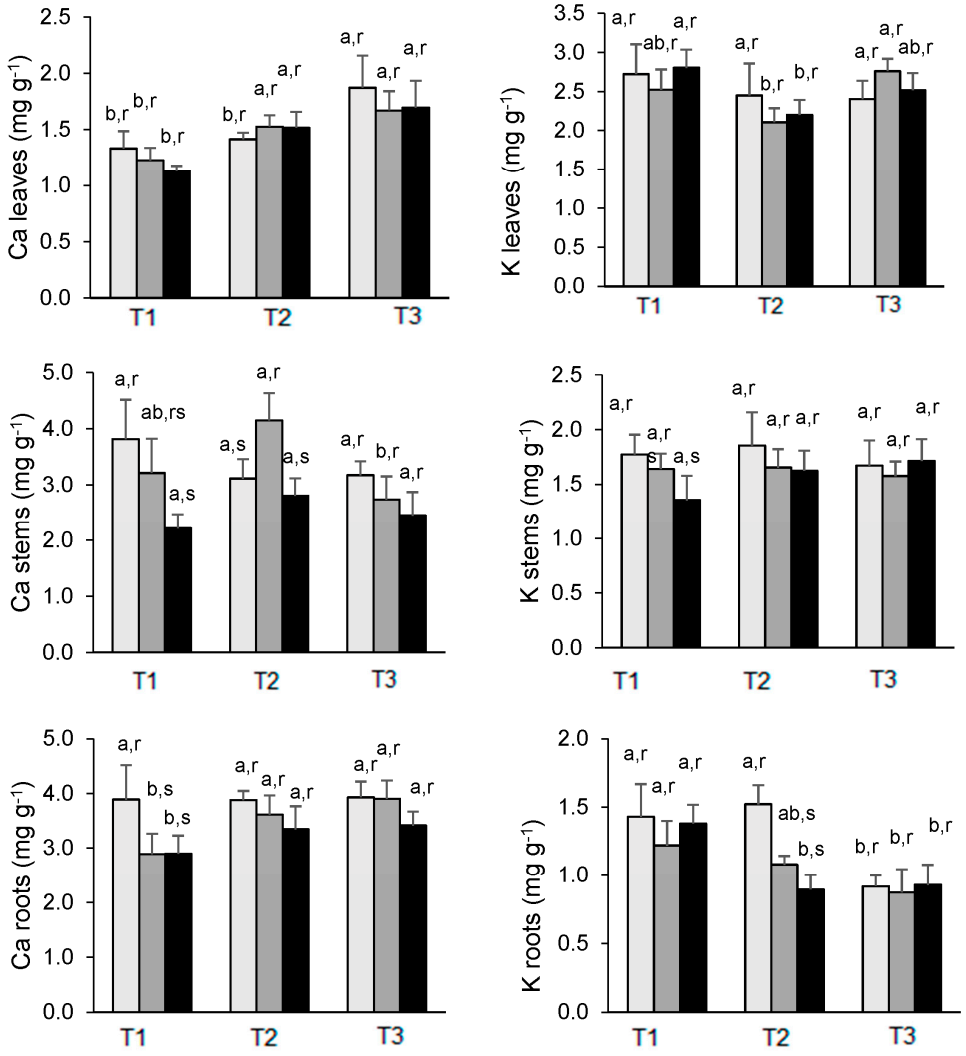

Figure 4. Changes in Ca (**left**) and K (**right**) concentration in the leaves, stems, and roots of *E. nitens* along the experiment. Mean values are expressed as mg g^{-1} ± standard deviation. For each element, different letters indicate significant differences at the 0.05 significance level over time (a, b) or between As treatments within each date (r, s). T1 = March; T2 = May; T3 = July: ☐ 0 µg As (Control), ☐ 100 µg As mL^{-1}, ■ 200 µg As mL^{-1}.

3.5.2. Potassium

The K concentrations were higher in leaves and stems than in roots. The levels of K in the roots of all treatments decreased from March to July, although the concentrations were alike on the last sampling date. In stems and leaves, the concentrations of K did not show significant differences between treatments on each date, except for stems in March between control and 200 As plants, the latter one showing a decline followed by a recovery in May and July (Figure 4). By the end of the experiment, the lowest levels in the leaves were measured in control plants with 2.40% compared with 2.76% of 100 As and 2.52% of 200 As-treated plants.

3.5.3. Iron

The accumulation of Fe by the different organs presents a pattern in the experiment, which is not unique. An increase in the Fe concentrations in the leaves was noted from March to July in As-treated plants, while in the same period, control plants declined from 111 μg g^{-1} to 93 μg g^{-1}. Furthermore, the increase of Fe in 200 As-treated plants is much more pronounced than in plants treated with half of this concentration—200 As plants had 242 μg g^{-1} Fe in July, whereas 100 As plants have 149 μg g^{-1} Fe (Figure 5).

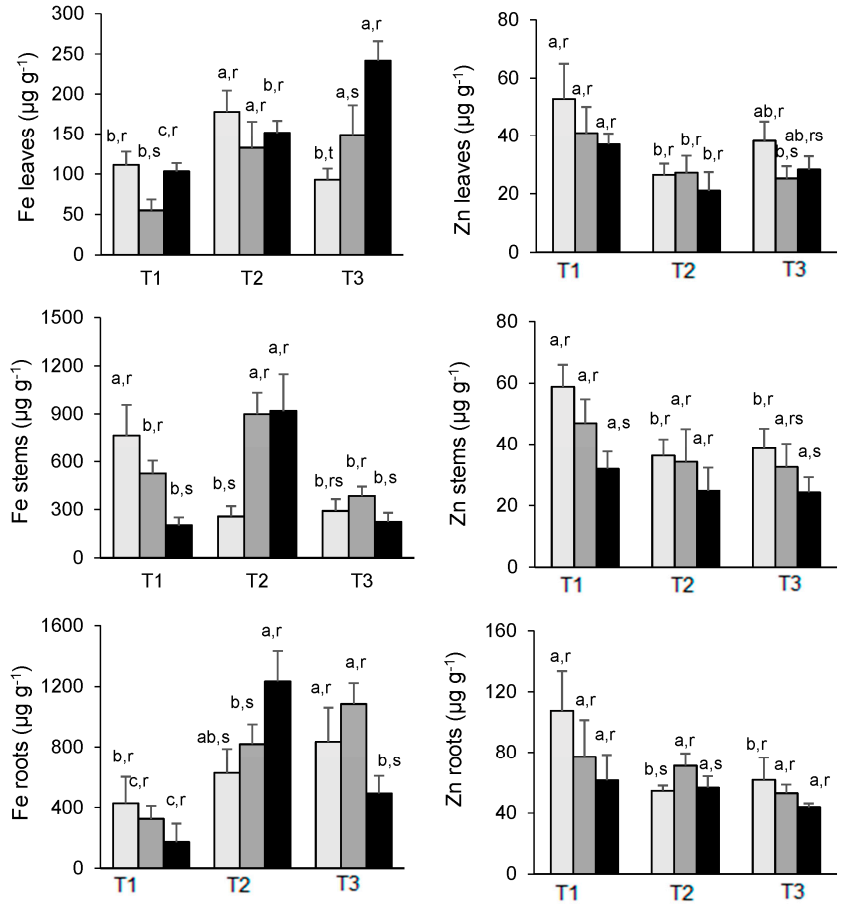

Figure 5. Changes in Fe (**left**) and Zn (**right**) concentration in the leaves, stems, and roots of *E. nitens* along the experiment. Mean values are expressed as mg g^{-1} ± standard deviation. For each element, different letters indicate significant differences at the 0.05 significance level over time (a, b, c) or between As treatments within each date (r, s). T1 = March; T2 = May; T3 = July: □ 0 μg As (Control), ■ 100 μg As mL^{-1}, ■ 200 μg As mL^{-1}.

Similarly to the roots, an increase in Fe uptake was also observed from March to July in both controls and 100 As plants, while in 200 As, a strong decline was verified from May to July, i.e., from 1233 μg g^{-1} Fe to 492 μg g^{-1} Fe. The accumulation of Fe by the stems is strongly affected by the As treatments in March, reaching a peak in May in the case of As treatments only, declining thereafter to concentrations lower than those verified in March, except for the 200 As plants which increase from 202 to 224 μg g^{-1} Fe between T1 (March) and T3 (July). Despite this variability, the roots are by far the main accumulator organ (Figure 5).

3.5.4. Zinc

The highest levels were found in the roots, while the stems and leaves exhibited similar concentrations. At T1 (March), there is a clear effect of the As concentrations used on the levels of Zn in the different organs compared with control plants. In May (T2), this trend is

slightly mitigated, while in July (T3), the Zn levels in control plants are higher than similar values observed in As-treated plant organs. For example, leaves from controls contained 38.2 μg g^{-1} Zn, while plants treated with 100 As and 200 As had 25.2 and 28.3 μg g^{-1} Zn, respectively. A similar result was observed in the root–control plants with 61.8 μg g^{-1} and 100 As and 200 As with 52.9 μg g^{-1} and 43.7 μg g^{-1}, respectively. This pattern, which is extensive to the stems, indicates a moderate antagonistic effect of As on the uptake of Zn and later translocation to the above-ground organs (Figure 5).

4. Discussion

4.1. As Accumulation and Plant Growth

It is well known that As might affect plant growth and development, and the negative impacts are usually attributed to As-promoted overproduction of reactive oxygen species (ROS) and, consequently, to the triggering of lipid peroxidation reactions and damage to cellular membranes. Yet, other major As impacts include changes in the availability of essential nutrients in photosynthesis and carbohydrate, lipid, protein, and sulfur metabolisms [47].

Different doses of As under the form of sodium arsenite (NaAsO2)—0.5, 1.0, 2.0, and 4.0 mg L^{-1} were supplied to *Eucalyptus camaldulensis* for 18 months, and it was observed that the As concentration increased in both roots and leaves, with increasing supplying doses [48]. For example, plants submitted to 0.5 mg L^{-1} contained 14.8 and 2.7 mg Kg^{-1} As in the roots and leaves, respectively, while plants treated with 4.0 mg L^{-1} presented in the same organs 37.2 and 6.6 mg Kg^{-1}.

Under hydroponic conditions, it was reported a maximum of 315 μg As g^{-1} in the roots and 10 μg g^{-1} As in the leaves of *E. grandis x E. urophylla*, after 14 days of exposure to 30 mg As L^{-1} in the form of Na_3AsO_4 [49]. This indicates that the availability in this medium is much more favorable than when soil cultures were used. In our case, using soil as substratum, the highest As concentration in the roots was 133 μg g^{-1} (see Table 1), when a concentration of 13 μg g^{-1} was also detected in the leaves.

The tested *Eucalyptus* species (*E. cladocalyx, E. melliodora, E. polybractea, E. viridis*) growing in gold mine tailings during five years, accumulate up to 5.1 μg g^{-1} As in mature leaves [50] leading the authors to conclude that the absence and/or tolerance of As effects on trees is a useful characteristic of a plant for phytostabilisation. In the same framework, the growth of 13 Eucalyptus clones in agricultural fields contaminated with As, Cd, Cr, Pb, Cu, and Zn [20] leads to an average value of 2.9 μg g^{-1} As, with a maximum of 7.8 μg g^{-1} As. The accumulation of As, Cu, Pb, and Zn was significantly higher in leaves than in stems and branches. Therefore, these findings clearly show that extrapolation from in vitro studies must be performed with great care since what happens in nature is not replicated in soil cultures or hydroponics [51,52].

The growth of *Eucalyptus camaldulensis* in highly contaminated sites (up to 1069 mg kg^{-1} of As and 4086 mg kg^{-1} of Pb) by a mine-spill in 1998, along the Guadiamar River valley (SW Spain), showed that the accumulation of these elements by *E. camaldulensis* leaves is relatively low, and below toxic levels, despite of its tolerance to a wide variety of soil conditions and rapid growth rate [53]. Thus, the variability of As accumulation by eucalyptus depends mainly on the type of experiment (soil or hydroponic cultures) and selected species beyond the time of exposure and As compound used. If the experimental assay is conducted in vivo, the type of the soil and its characteristics and climatic conditions are of extreme importance.

4.2. As Interaction with Macro and Micronutrients

The whole elements studied are crucial to plants with the following adequate concentrations in dry tissues: 0.5%, 1.0%, 100 mg Kg^{-1}, and 20 mg Kg^{-1}, respectively [54]. Their role in plant metabolism is diverse. For example, Fe is taken up as Fe^{2+} and is needed for chlorophyll synthesis and a cofactor for redox enzymes and electron transport chain carriers, while Zn is taken up as Zn^{2+} and is required for protein breakdown and enzyme activation [55]. Calcium has a main structural role in the cell wall and membranes, it is a

counter-cation for anions in the vacuole, and the cytosolic Ca^{2+} concentration is an important intracellular messenger [56], also having a crucial role in the good performance of the photosynthetic apparatus and in other elemental balance [57], while K which is abundantly present in the cytosol participates in enzyme activation, protein synthesis, osmoregulation, ionic balance, photosynthesis, stomata functioning and also stress resistance [58].

The response of *Pteris cretica* and *Spinacia oleracea* shoots to As(V) treatments (soil was artificially contaminated with 20 and 100 mg/kg) showed that the highest treatment affected growth, and Fe and Zn content in *S. oleracea* but not in *P. cretica* where an increase in the concentrations of these elements was observed, compared with control data [59], which is related with the status of *P. cretica* (As-hyperaccumulator) vis a vis the status of *S. oleracea* (As-root excluder).

The interaction of As with Fe was assessed through the hydroponic of barley for two weeks [60]. It was observed a decline both in the Chl. index and in the Fe concentration of the As-treated plant shoots, beyond a decline of P, K, Ca, Mg, Mn, Zn, and Cu concentrations. Conversely, Yu et al. [61], when studying the effects of iron fertilizer on two cultivars of *Ipomoea aquatica* grown in As-contaminated soils at different As concentrations, observed that the use of the fertilizer causes a significant reduction in the uptake of As, thus enhancing plant growth.

In our case, it seems to occur a continuous enrichment of the Fe content of the leaves throughout the experiment in parallel with a decrease in the roots of the plants treated with 200 As, whereas in a previous study with *Eucalyptus globulus* [24], a decrease in the same organ was noted as a result of As treatments. Such Fe enrichment is in agreement with the increase in the levels of both total chlorophyll and carotenoids in our As-treated plants due to the important role of Fe for chlorophyll biosynthesis [55]. It should be noted that although the overwhelming majority of the studies reported that As inhibits the synthesis (or promote the degradation) of photosynthetic pigments [47,60,62,63], in a few cases, it was noted a neutral effect of As or even a stimulus [64,65].

For example, in tomato (*Lycopersicon esculentum*) cultivated on soils contaminated with sublethal doses of As (15, 25, 50, and 100 mg kg^{-1}), it was observed that the two lower doses stimulated the synthesis of pigments, while the two higher doses had an antagonist effect [62], whereas the growth of *Tamarix gallica* (halophytic shrub) for three months in the presence 0, 200, 500, and 800 µM As demonstrates that the levels of total chlorophylls and carotenoids did not vary significantly, despite the increase of As concentration. With 800 µM, symptoms of toxicity appear, affecting only the growth but not the nutrient contents [65]. These data indicate that the variability in the response depends on the plant species, the As concentrations and the chemical species of the element beyond characteristics of experimental conditions.

An antagonistic relationship between Zn and As seems to exist, i.e., in soils, Zn was found to reduce As availability and the accumulation in *Ipomoea aquatica*, particularly under high levels of Zn—3 mg/L [66], which agrees with our results since the overwhelming Zn levels in the different organs are higher in control than in As treated plants.

The fern *Pteris vittata* is a hyperaccumulator of As, and thus, several attempts have been made to understand how the high levels of As influence the distribution of both macro and micronutrients in the plant. In this context, the plant has been submitted to increasing levels of As applied to the soil (from 0 to 500 mg As kg^{-1}) for 6 months [67]. In what concerns the interaction between As and K, it was verified that the young fronds had the highest K concentrations while the old fronds had the lowest ones. Moreover, at higher As levels, an enrichment in K in the fronds was observed to balance excessive anions caused by As hyperaccumulation [67], which agrees with our results since, at the end of the experiment, the lowest levels in the *E. nitens* leaves were measured in control plants with 2.40% compared with 2.76% of 100 µg As mL^{-1} and 2.52% of 200 µg As mL^{-1} treated plants.

Previous studies by energy dispersive X-ray spectroscopy revealed that the exposure to As (III) significantly reduced the S, Si, Cl, K, Ca, Fe, and Cu concentrations in rice roots [68],

also slightly limiting the concentration of important elements in the rice shoots. It seems that As interferes with the uptake of nutrients (micro and macro) through competition for binding to uptake carriers [69], beyond the differences among plant species, forms of As and concentrations used, and time of exposition.

4.3. As Impact on the Performance of the Photosynthetic Apparatus

The performance of the photosynthetic apparatus showed only minor, if any, impacts on the first date of the evaluation (Figure 2 and Table 2). Yet, a gradual impact was observed with time; in May, after 4 months of As exposure, P_n significantly declined only under maximal exposure (200 As plants), which was in accordance with the reduction in the use of energy through photochemistry ($Y_{(II)}$, q_L). Such P_n reduction seemed to be closely associated with the large stomatal closure (which also led to an E decline) but not with impacts on the PSII performance, as revealed by an absence of significant changes in the PSII photochemical efficiency (F_v/F_m, F_v'/F_m'), PSII inactivation (F_s/F_m'), photoprotective thermal dissipation ($Y_{(NPQ)}$, q_N) or in the photoinhibition indexes. In the same context, a reduction in the CO_2 assimilation rate was associated with decreased stomatal conductance, transpiration rate, and intercellular CO_2 concentration in soybean treated with both As(III) and As(V). The changes noted in the photochemical phase of photosynthesis suggest a reduction in electron transport, mainly under As(V) treatment [70]. Furthermore, the reduction of stomatal conductance, the inhibition of photosynthesis, the degradation of the chlorophyllin pigments, the reduction of ATP synthesis, the chloroplast membrane disintegration as well as the activation of antioxidative enzymes as a response to the overproduction of Reactive Oxygen Species (ROS), are the main physiological processes as a result of the injurious effects of As [71].

Until May, our F_v/F_m values were similar regardless of the treatments, with values around 0.8, which agree with Björkman and Demmig [72], which indicate that the F_v/F_m ratio is nearly constant in unstressed leaves. Nevertheless, in July, a reduction of 9.1% in the F_v/F_m value was noted in plants treated with 200 As compared with control and 100 As, which can be indicative of smooth stress. Zemanová et al. [64] observed a decrease of F_v/F_m values in both young and old fronds of the As hyperaccumulator *Pteris cretica* L. when treated with 100 mg As per kg soil and 250 mg As per kg soil -with 100 As the decrease ranges between 12.5% and 14.3%, for young and old fronds, respectively, climbing to 29% in old fronds treated with 250 As, thus indicating a faster progression of senescence in the latter case.

The growth of *F. tikoua* leaves was significantly inhibited at As concentrations higher than 80 µmol/L in solution. Concentrations such as 320 and 480 µmol/L resulted in significant decreases in the maximum quantum efficiency of photosystem II (PSII) (F_v/F_m), variable to initial chlorophyll fluorescence (F_v/F_o), and quantum yield of PSII electron transport (Y(II)) of *F. tikoua* leaves, whereas significantly higher non-photochemical and photochemical quenching of fluorescence values were found at 160, 320, and 480 µmol/L As, indicating that PSII reaction centers were damaged and that the plant eliminates excess energy stress on the photochemical apparatus as a possible adaptation mechanism [73].

With 6 months of As exposure, 100 As plants showed values of gas exchanges and fluorescence parameters without significant differences when compared with control plants, with a few exceptions regarding P_n, $Y_{(II)}$, and q_L data. However, the 200 As plants showed additional impacts by the end of the experiment, similar to those reported in *E. globulus* submitted to the same As treatment [24]. In fact, the 200 As plants of *E. nitens* showed the maximal P_n reduction of the entire experiment, which was accompanied by a decline in the use of energy through photochemical processes ($Y_{(II)}$, q_L) but also with significant impacts in the PSII, as reflected in the drop of photochemical efficiency (F_v/F_m), and a greater inactivation status (F_s/F_m'). Still, As did not cause increases in the photoinhibition indexes (PI_{Dyn}, PI_{Chr}, PI_{Total}) and in $Y_{(NO)}$. This latter parameter is usually stable even under environmentally stressful conditions [73]. However, its increase reflects the growing importance of the non-photochemical quenching processes associated with photoinactivation and non-

regulated energy (heat and fluorescence) dissipation at the PSII level [36,40,74]. In this way, the maintenance of $Y_{(NO),}$ even in the 200 As plants after 6 months of As exposure, suggests that, despite the reduction of photochemical energy conversion ($Y_{(II)}$), the energy dissipation through non-photochemical processes in PSII($Y_{(NPQ)}$), which is usually associated with the protective down-regulation of light-harvesting function [40], was capable of minimize the PSII impacts, in contrast with *Pisum sativum* Pb-treated plants, where photoprotective mechanisms (evaluated through NPQ) were suppressed [75]. Moreover, q_N and NPQ were found to increase in barley seedlings exposed to Cu (80 μM) during six days but decreased under a Fe (1.5 mM) treatment, thus indicating different action mechanisms/impacts [76]. Therefore, our findings denoted the capability of the photosynthetic machinery of *E. nitens* to respond and cope with high levels of As to a certain extent.

Furthermore, since *E. nitens* is high tolerance to frost, as recognized by Gomes and Canhoto [27], this plant can be used as an alternative in phytoremediation processes in some mining abandoned areas of northern Portugal where winter temperatures are too low and impeditive to an efficient uptake and/or translocation mechanism of major heavy metals or metalloids present in the substrata. It is worth emphasizing the abandoned mines of Jales (gold production), Borralha (tungsten production), and Montesinho (tin production), all of them located in northern areas [77].

5. Conclusions

Roots are unquestionably the main accumulator organs, reaching a peak in both treatments in May, with 90.1 μg g^{-1} and 133 μg g^{-1} for plants treated with 100 As and 200 As, respectively, declining thereafter. The translocation to the leaves reaches a maximum of 15.9 and 14.0 μg g^{-1} for plants treated with 100 As and 200 As, respectively, showing that in the current experimental conditions and taking into account the Bioaccumulation Factor, always >1, the below-ground organs were efficient in the extraction of As from the matrix. The performance of the photosynthetic apparatus showed a gradual impact with time in some gas exchange parameters such as net photosynthetic rate (P_n), stomatal conductance to H_2O (g_s), and the transpiration rate (E), particularly with the use of 200 As, but without impacting with significant changes the PSII performance, i.e., the PSII photochemical efficiency, the PSII inactivation or the photoprotective thermal dissipation. The highest levels of As seem to stimulate the accumulation of Fe in the leaves, which is in agreement with the increase of total chlorophyll in both As-treated plants compared with control plants. Regarding the effects of As on Zn levels, it seems to exist a moderate antagonistic effect on the uptake of Zn and later translocation to the above-ground organs, which is more pronounced with the highest As treatment. In general, this species is able to cope with As-contaminated substrate surrounding mining areas, although the As extraction by the root system would be expected to be slower than that monitored in soil pots.

Author Contributions: Conceptualization, F.H.R. and F.C.L.; formal analysis, F.H.R., F.C.L., J.P., M.G. and J.C.R.; funding acquisition, F.H.R. and F.C.L.; investigation, J.C.R., F.H.R., F.C.L. and J.P.; methodology, F.H.R., F.C.L., J.C.R. and M.G.; project administration, F.H.R. and F.C.L.; supervision, F.H.R., F.C.L. and J.C.R.; writing—original draft, F.H.R. and J.C.R.; writing—review and editing, F.H.R., F.C.L., J.C.R., M.M.A.S. and M.M.S. All authors have read and agreed to the published version of the manuscript.

Funding: This work received funding support from national funds from Fundação para a Ciência e a Tecnologia, I.P. (FCT), Portugal, through the research units UIDB/04035/2020 (GeoBioTec), UIDB/00239/2020 (CEF), and UID/FIS/04559/2020 (LIBPhys), as well as LA/P/0092/2020 (Associate Laboratory TERRA).

Data Availability Statement: All relevant data are included in the manuscript.

Acknowledgments: The authors would like to thank Viveiros do Furadouro (Grupo Altri), particularly Engª Ivone Neves, for gracious access to *Eucalyptus nitens* plants.

Conflicts of Interest: The authors have no financial or non-financial interest to disclose.

References

1. European Environment Agency (EEA). *EMEP/EEA Air Pollutant Emission Inventory Guidebook 2019*; Technical Guidance to Prepare National Emission Inventories; Publication Office of the European Union: Luxembourg, 2019. [CrossRef]
2. Reboredo, F.H.; Pelica, J.; Lidon, F.C.; Ramalho, J.C.; Pessoa, M.F.; Calvão, T.; Simões, M.; Guerra, M. Heavy metal content of edible plants collected close to an area of intense mining activity (southern Portugal). *Environ. Monit. Assess.* **2018**, *190*, 484. [CrossRef]
3. Carrondo, M.; Reboredo, F.; Ganho, R.; Santos Oliveira, J.F. Heavy metal analysis of sediments in Tejo estuary, Portugal, using a rapid flameless atomic absorption procedure. *Talanta* **1984**, *31*, 561–564. [CrossRef]
4. Reboredo, F.H.S.; Ribeiro, C.A.G. Vertical distribution of Al, Cu, Fe and Zn in soil salt marshes of the Sado estuary, Portugal. *Int. J. Environ. Stud.* **1984**, *23*, 249–253. [CrossRef]
5. Martins, M.V.A.; Laut, L.; Duleba, W.; Zaaboub, N.; Aleya, L.; Terroso, D.L.; Sequeira, C.; Pena, A.; Rodrigues, M.A.; Rocha, F. Sediment quality and possible uses of dredged materials: The Ria de Aveiro lagoon mouth area (Portugal). *J. Sediment Environ.* **2017**, *2*, 149–166. [CrossRef]
6. Ferreira, J.; Lopes, D.; Rafael, S.; Relvas, H.; Almeida, S.M.; Miranda, A.I. Modelling air quality levels of regulated metals: Limitations and challenges. *Environ. Sci. Pollut. Res.* **2020**, *27*, 33916–33928. [CrossRef]
7. Tomiyama, S.; Igarashi, T. The potential threat of mine drainage to groundwater resources. *Curr. Opin. Environ. Sci. Health.* **2022**, *27*, 100347. [CrossRef]
8. Eurostat, Waste Statistics. 2018. Available online: https://ec.europa.eu/eurostat/statistics-explained/index.php?title=Waste_statistics#Total_waste_generation (accessed on 16 July 2022).
9. Reboredo, F.; Henriques, F. Some observations on the leaf ultrastructure of *Halimione portulacoides* (L.) Aellen grown in a medium containing copper. *J. Plant Physiol.* **1991**, *137*, 717–722. [CrossRef]
10. Yruela, I. Copper in plants: Acquisition, transport and interactions. *Funct. Plant Biol.* **2009**, *36*, 409–430. [CrossRef]
11. Chen, G.; Li, J.; Han, H.; Du, R.; Wang, X. Physiological and molecular mechanisms of plant responses to copper stress. *Int. J. Mol. Sci.* **2022**, *23*, 12950. [CrossRef]
12. Ngole-Jeme, V.M.; Fantke, P. Ecological and human health risks associated with abandoned gold mine tailings contaminated soil. *PLoS ONE* **2017**, *12*, e0172517. [CrossRef]
13. Xiao, M.; Xu, S.; Yang, B.; Zeng, G.; Qian, L.; Huang, H.; Ren, S. Contamination, source apportionment, and health risk assessment of heavy metals in farmland soils surrounding a typical copper tailings pond. *Int. J. Environ. Res. Public Health* **2022**, *19*, 14264. [CrossRef]
14. European Commission. *Guidelines for Mine Closure Activities and Calculation and Periodic Adjustment of Financial Guarantees*; Publications Office of the European Union: Luxembourg, 2021; 216p.
15. DeCarb/Interreg Europe. *Needs Analysis Report on Environmental Restitution and Land Restoration in Decarb Regions*; Ministry of Economic Affairs, Labour and Energy: Brandenburg, 2019; 120p, Available online: https://projects2014-2020.interregeurope.eu/fileadmin/user_upload/tx_tevprojects/library/file_1580819578. (accessed on 20 October 2022).
16. Dradrach, A.; Karczewska, A.; Szopka, K.; Lewińska, K. Accumulation of arsenic by plants growing in the sites strongly contaminated by historical mining in the Sudetes region of Poland. *Int. J. Environ. Res. Public Health* **2020**, *17*, 3342. [CrossRef]
17. Durante-Yánez, E.V.; Martínez-Macea, M.A.; Enamorado-Montes, G.; Combatt Caballero, E.; Marrugo-Negrete, J. Phytoremediation of soils contaminated with heavy metals from gold mining activities using *Clidemia sericea* D. Don. *Plants* **2022**, *11*, 597. [CrossRef]
18. Mleczek, M.; Goliński, P.; Krzesłowska, M.; Gąsecka, M.; Magdziak, Z.; Rutkowski, P.; Budzyńska, S.; Waliszewska, B.; Kozubik, T.; Karolewski, Z.; et al. Phytoextraction of potentially toxic elements by six tree species growing on hazardous mining sludge. *Environ. Sci. Pollut. Res.* **2017**, *24*, 22183–22195. [CrossRef]
19. Mourinha, C.; Palma, P.; Alexandre, C.; Cruz, N.; Rodrigues, S.M.; Alvarenga, P. Potentially toxic elements'contamination of soils affected by mining activities in the Portuguese sector of the Iberian Pyrite Belt and optional remediation actions: A review. *Environments* **2022**, *9*, 11. [CrossRef]
20. Oliveira, L.W. Phytoremediation in Portugal: A Comparison between Plants and Different Wastewaters. Master's Thesis, Biologia e Gestão da Qualidade da Água, Departamento de Biologia da Faculdade de Ciências da Universidade do Porto, Porto, Portugal, 2021; 123p.
21. Yan, A.; Wang, Y.; Tan, S.N.; Yusof, M.L.M.; Ghosh, S.; Chen, Z. Phytoremediation: A promising approach for revegetation of heavy metal-polluted land. *Front. Plant Sci.* **2020**, *11*, 359. [CrossRef]
22. Mughini, G.; Alianiello, F.; Benedetti, A.; Gras, L.M.; Gras, M.A.; Salvati, L. Clonal variation in growth, arsenic and heavy metal uptakes of hybrid *Eucalyptus* clones in a Mediterranean environment. *Agrofor. Syst.* **2013**, *87*, 755–766. [CrossRef]
23. Xing, Z.; Wang, Z.; Zhang, C.; He, W.; Luo, J. Balance between soil remediation and economic benefits of *Eucalyptus globulus*. *Bull. Environ. Contam. Toxicol.* **2019**, *102*, 887–891. [CrossRef]
24. Reboredo, F.H.; Pelica, J.; Lidon, F.C.; Pessoa, M.F.; Silva, M.M.; Guerra, M.; Leitão, R.; Ramalho, J.C. The tolerance of *Eucalyptus globulus* to soil contamination with arsenic. *Plants* **2021**, *10*, 627. [CrossRef]

25. El Rasafi, T.; Pereira, R.; Pinto, G.; Gonçalves, F.J.M.; Haddioui, A.; Ksibi, M.; Rombke, J.; Sousa, J.P.; Marques, C.R. Potential of *Eucalyptus globulus* for the phytoremediation of metals in a Moroccan iron mine soil—A case study. *Environ. Sci. Pollut. Res.* **2021**, *28*, 15782–15793. [CrossRef]
26. Reboredo, F.; Pais, J. Evolution of forest cover in Portugal—A review of the 12th–20th centuries. *J. For. Res.* **2014**, *25*, 249–256. [CrossRef]
27. Gomes, F.; Canhoto, J.M. Micropropagation of *Eucalyptus nitens* Maiden (Shining Gum). *In Vitro Cell Dev. Biol. Plant* **2003**, *39*, 316–321. [CrossRef]
28. Reboredo, F.; Lidon, F. UV-B radiation effects on terrestrial plants—A perspective. *Emir. J. Food Agric.* **2012**, *24*, 502–509. [CrossRef]
29. Iriel, A.; Dundas, G.; Cirelli, A.F.; Lagorio, M.G. Effect of arsenic on reflectance spectra and chlorophyll fluorescence of aquatic plants. *Chemosphere* **2015**, *119*, 697–703. [CrossRef] [PubMed]
30. Kalaji, H.M.; Jajoo, A.; Oukarroum, A.; Brestic, M.; Zivcak, M.; Samborska, I.A.; Cetner, M.D.; Lukasik, I.; Goltsev, V.; Ladle, R.J. Chlorophyll a fluorescence as a tool to monitor physiological status of plants under abiotic stress conditions. *Acta Physiol. Plant.* **2016**, *38*, 102. [CrossRef]
31. IPMA. Instituto Português do Mar e da Atmosfera (IPMA). 2016. Available online: http://www.ipma.pt/pt/index.html (accessed on 18 July 2022).
32. Lambers, H.; Poorter, H. Inherent variation in growth rate between higher plants: A search for physiological causes and ecological consequences. *Adv. Ecol. Res.* **2004**, *34*, 283–362. [CrossRef]
33. Lichtenthaler, H. Chlorophylls carotenoids and carotenoids: Pigments of photosynthetic biomembranes. *Methods Enzimol.* **1987**, *148*, 350–382. [CrossRef]
34. Rodrigues, W.P.; Martins, M.Q.; Fortunato, A.S.; Rodrigues, A.P.; Semedo, J.N.; Simões-Costa, M.C.; Pais, I.P.; Leitão, A.E.; Colwell, F.; Goulão, L.; et al. Long-term elevated air [CO_2] strengthens photosynthetic functioning and mitigates the impact of supra-optimal temperatures in tropical *Coffea arabica* and *Coffea canephora* species. *Glob. Chang. Biol.* **2016**, *22*, 415–431. [CrossRef]
35. Semedo, J.N.; Rodrigues, A.P.; Lidon, F.C.; Pais, I.P.; Marques, I.; Gouveia, D.; Armengaud, J.; Silva, M.J.; Martins, S.; Semedo, M.C.; et al. Intrinsic non-stomatal resilience to drought of the photosynthetic apparatus in *Coffea* spp. is strengthened by elevated air [CO_2]. *Tree Physiol.* **2021**, *41*, 708–727. [CrossRef]
36. Kramer, D.M.; Johnson, G.; Kiirats, O.; Edwards, G.E. New flux parameters for the determination of Q_A redox state and excitation fluxes. *Photosynth. Res.* **2004**, *79*, 209–218. [CrossRef]
37. Krause, G.H.; Jahns, P. Non-photochemical energy dissipation determined by chlorophyll fluorescence quenching: Characterization and function. In *Chlorophyll a Fluorescence: A Signature of Photosynthesis*; Govindjee, G.C.P., Ed.; Springer: Dordrecht, The Netherlands, 2004; pp. 463–495.
38. Klughammer, C.; Schreiber, U. Complementary PS II quantum yields calculated from simple fluorescence parameters measured by PAM fluorometry and the Saturation Pulse method. *PAM Appl. Notes* **2008**, *1*, 27–35.
39. Stirbet, A.; Govindjee. On the relation between the Kautsky effect (chlorophyll *a* fluorescence induction) and Photosystem II: Basics and applications of the OJIP fluorescence transient. *J. Photochem. Photobiol. B Biol.* **2011**, *104*, 236–257. [CrossRef] [PubMed]
40. Huang, W.; Zhang, S.-B.; Cao, K.-F. Cyclic electron flow plays an important role in photoprotection of tropical trees illuminated at temporal chilling temperature. *Plant Cell Physiol.* **2011**, *52*, 297–305. [CrossRef] [PubMed]
41. Werner, C.; Correia, O.; Beyschlag, W. Characteristic patterns of chronic and dynamic photoinhibition of different functional groups in a Mediterranean ecosystem. *Funct. Plant Biol.* **2002**, *29*, 999–1011. [CrossRef] [PubMed]
42. Martins, M.Q.; Rodrigues, W.P.; Fortunato, A.S.; Leitão, A.E.; Rodrigues, A.P.; Pais, I.P.; Martins, L.D.; Silva, M.J.; Reboredo, F.H.; Partelli, F.L.; et al. Protective response mechanisms to heat stress in interaction with high [CO_2] conditions in *Coffea* spp. *Front. Plant Sci.* **2016**, *7*, 947. [CrossRef]
43. EPA. *Field Portable X-ray Fluorescence Spectrometry for the Determination of Elemental Concentration in Soil and Sediment*; Method 6200; U.S. Environmental Protection Agency (EPA): Washington, DC, USA, 2007. Available online: https://www.epa.gov/sites/default/files/2015-12/documents/6200.pdf (accessed on 10 October 2022).
44. NRCan. TILL-1, TILL-2, TILL-3 and TILL-4. In *Geochemical Soil and Till Reference Materials*; Natural Resources Canada: Ottawa, ON, Canada, 1995.
45. Pessanha, S.; Guilherme, A.; Carvalho, M.L. Comparison of matrix effects on portable and stationary XRF spectrometers for cultural heritage samples. *Appl. Phys. A* **2009**, *97*, 497–505. [CrossRef]
46. Gallardo, H.; Queralt, I.; Tapias, J.; Guerra, M.; Carvalho, M.L.; Margúi, E. Possibilities of low-power X-ray fluorescence spectrometry methods for rapid multielemental analysis and imaging of vegetal foodstuffs. *J. Food Compos. Anal.* **2016**, *50*, 1–9. [CrossRef]
47. Zhang, J.; Hamza, A.; Xie, Z.; Hussain, S.; Brestic, M.; Tahir, M.A.; Ulhassan, Z.; Yu, M.; Allakhverdiev, S.I.; Shabala, S. Arsenic transport and interaction with plant metabolism: Clues for improving agricultural productivity and food safety. *Environ. Pollut.* **2021**, *290*, 117987. [CrossRef]
48. Ahmad, F.D.; Ahmad, N.; Masood, K.R.; Hussain, M.; Malik, M.F.; Qayyum, A. Phytoremediation of arsenic-contaminated soils by *Eucalyptus camaldulensis*, *Terminalia arjuna* and *Salix tetrasperma*. *J. Appl. Bot. Food Qual.* **2018**, *91*, 8–13. [CrossRef]

49. Wang, W.; Meng, M.; Li, L. Arsenic detoxification in Eucalyptus: Subcellular distribution, chemical forms, and sulfhydryl substances. *Environ. Sci. Pollut. Res.* **2019**, *26*, 24372–24379. [CrossRef]
50. King, D.J.; Doronila, A.I.; Feenstra, C.; Baker, A.J.; Woodrow, I.E. Phytostabilisation of arsenical gold mine tailings using four Eucalyptus species: Growth, arsenic uptake and availability after five years. *Sci. Total Environ.* **2008**, *406*, 35–42. [CrossRef] [PubMed]
51. Reboredo, F. Copper and zinc uptake by *Halimione portulacoides* (L.). A long-term accumulation experiment. *Bull. Environ. Contam. Toxicol.* **1991**, *46*, 442–449. [CrossRef]
52. Reboredo, F. Interaction between copper and zinc and their uptake by *Halimione portulacoides* (L.) Aellen. *Bull. Environ. Contam. Toxicol.* **1994**, *52*, 598–605. [CrossRef] [PubMed]
53. Madejón, P.; Marañón, T.; Navarro-Fernández, C.M.; Domínguez, M.T.; Alegre, J.M.; Robinson, B.; Murillo, J.M. Potential of *Eucalyptus camaldulensis* for phytostabilization and biomonitoring of trace-element contaminated soils. *PLoS ONE* **2017**, *12*, e0180240. [CrossRef] [PubMed]
54. Evert, R.F.; Eichhorn, S.E.; Raven, P.H. *Raven Biology of Plants*, 8th ed.; W.H. Freeman and Company Publishers: New York, NY, USA, 2013; 727p.
55. Rai, S.; Singh, P.K.; Mankotia, S.; Swain, J.; Satbhai, S.B. Iron homeostasis in plants and its crosstalk with copper, zinc, and manganese. *Plant Stress* **2021**, *1*, 100008. [CrossRef]
56. Thor, K. Calcium—Nutrient and messenger. *Front. Plant Sci.* **2019**, *10*, 440. [CrossRef] [PubMed]
57. Ramalho, J.C.; Rebelo, M.C.; Santos, M.E.; Antunes, M.L.; Nunes, M.A. Effects of calcium deficiency on *Coffea arabica*. Nutrient changes and correlations of calcium levels with some photosynthetic parameters. *Plant Soil* **1995**, *172*, 87–96. [CrossRef]
58. Pandey, G.K.; Mahiwal, S. *Role of Potassium in Plants*; Springer Briefs in Plant Science Book Series; Springer International Publishing: Berlin/Heidelberg, Germany, 2020; 81p. [CrossRef]
59. Zemanová, V.; Pavlíková, D.; Hnilička, F.; Pavlík, M. Arsenic toxicity-induced physiological and metabolic changes in the shoots of *Pteris cretica* and *Spinacia oleracea*. *Plants* **2021**, *10*, 2009. [CrossRef]
60. Shaibur, M.R.; Kitajima, N.; Huq, S.M.I.; Kawai, S. Arsenic-iron interaction: Effect of additional iron on arsenic-induced chlorosis in barley grown in water culture. *Soil Sci. Plant Nutr.* **2009**, *55*, 739–746. [CrossRef]
61. Yu, T.-H.; Peng, Y.-Y.; Lin, C.-X.; Qin, J.-H.; Li, H.-S. Application of iron and silicon fertilizers reduces arsenic accumulation by two *Ipomoea aquatica* varieties. *J. Integr. Agric.* **2016**, *15*, 2613–2619. [CrossRef]
62. Chandrakar, V.; Naithani, S.C.; Keshavkant, S. Arsenic-induced metabolic disturbances and their mitigation mechanisms in crop plants: A review. *Biologia* **2016**, *71*, 367–377. [CrossRef]
63. Zemanová, V.; Popov, M.; Pavlíková, D.; Kotrba, P.; Hnilička, F.; Česká, J.; Pavlík, M. Effect of arsenic stress on 5-methylcytosine, photosynthetic parameters and nutrient content in arsenic hyperaccumulator *Pteris cretica* (L.) var. Albo-lineata. *BMC Plant Biol.* **2020**, *20*, 130. [CrossRef] [PubMed]
64. Miteva, E. Accumulation and effect of arsenic on tomatoes. *Commun. Soil Sci. Plant Anal.* **2002**, *33*, 1917–1926. [CrossRef]
65. Sghaier, D.B.; Duarte, B.; Bankaji, I.; Caçador, I.; Sleimi, N. Growth, chlorophyll fluorescence and mineral nutrition in the halophyte *Tamarix gallica* cultivated in combined stress conditions: Arsenic and NaCl. *J. Photochem. Photobiol. B Biol.* **2015**, *149*, 204–214. [CrossRef] [PubMed]
66. Sanchary, I.J.; Huq, S.M.I. Remediation of arsenic toxicity in the soil-plant system by using zinc fertilizers. *J. Agric. Chem. Environ.* **2017**, *6*, 30–37. [CrossRef]
67. Tu, C.; Ma, L.Q. Effects of arsenic on concentration and distribution of nutrients in the fronds of the arsenic hyperaccumulator *Pteris vittata* L. *Environ. Pollut.* **2005**, *135*, 333–340. [CrossRef] [PubMed]
68. Singh, R.; Upadhyay, A.K.; Singh, D.P. Regulation of oxidative stress and mineral nutrient status by selenium in arsenic treated crop plant *Oryza sativa*. *Ecotoxicol. Environ. Saf.* **2018**, *148*, 105–113. [CrossRef]
69. Gusman, G.S.; Oliveira, J.A.; Farnese, F.S.; Cambraia, J. Mineral nutrition and enzymatic adaptation induced by arsenate and arsenite exposure in lettuce plants. *Plant Physiol. Biochem.* **2013**, *71*, 307–314. [CrossRef]
70. Vezza, M.E.; Alemano, S.; Agostini, E.; Talano, M.A. Arsenic toxicity in soybean plants: Impact on chlorophyll fluorescence, mineral nutrition and phytohormones. *J. Plant Growth Regul.* **2021**, *41*, 2719–2731. [CrossRef]
71. Abbas, G.; Murtaza, B.; Bibi, I.; Shahid, M.; Niazi, N.K.; Khan, M.I.; Amjad, M.; Hussain, M.; Natasha. Arsenic uptake, toxicity, detoxification, and speciation in plants: Physiological, biochemical, and molecular aspects. *Int. J. Environ. Res. Public Health* **2018**, *15*, 59. [CrossRef]
72. Björkman, O.; Demmig, B. Photon yield of O_2 evolution and chlorophyll fluorescence characteristics at 77 K among vascular plants of diverse origins. *Planta* **1987**, *17*, 489–504. [CrossRef] [PubMed]
73. Yong, W.; Chai, L.; Yang, Z.; Mubarak, H.; Tang, C. Chlorophyll fluorescence in leaves of *Ficus tikoua* under arsenic stress. *Bull. Environ. Contam. Toxicol.* **2016**, *97*, 576–581. [CrossRef]
74. Busch, F.; Hunter, N.P.A.; Ensminger, I. Biochemical constrains limit the potential of the photochemical reflectance index as a predictor of effective quantum efficiency of photosynthesis during the winter-spring transition in Jack pine seedlings. *Funct. Plant Biol.* **2009**, *36*, 1016–1026. [CrossRef] [PubMed]
75. Kycko, M.; Romanowska, E.; Zagajewski, B. Lead-induced changes in fluorescence and spectral characteristics of pea leaves. *Remote Sens.* **2019**, *11*, 1885. [CrossRef]

76. Lysenko, E.A.; Klaus, A.A.; Kartashov, A.V.; Kusnetsov, V.V. Specificity of Cd, Cu, and Fe effects on barley growth, metal contents in leaves and chloroplasts, and activities of photosystem I and photosystem II. *Plant Physiol. Biochem.* **2020**, *147*, 191–204. [CrossRef] [PubMed]
77. Carvalho, J.M.F.; Diamantino, C.; Rosa, C.J.P.; Carvalho, E. Potential recovery of mineral resources from mining tailings of abandoned mines in Portugal. In Proceedings of the 3rd International Symposium on Enhanced Landfill Mining, Lisbon, Portugal, 8–10 February 2016; pp. 501–516.